Accurate Radar Cross Section Modelling of Jet Inlets & Engines

Kwok Kee Chan
Chan Technologies Inc.
15 Links Lane
Brampton, Ontario L6Y 5H1
Canada

Silvester Wong and Edwin Riseborough
DRDC-Ottawa
3701 Carling Avenue
Ottawa, Ontario K1A 0Z4
Canada

kwok-kee.chan@rogers.com / Silvester.Wong@drdc-rddc.gc.ca / Ed.Riseborough@drdc-rddc.gc.ca

SUMMARY

Most of the industrial software codes used for the prediction of the radar cross-section (RCS) of aircrafts are based on ray tracing. While ray based methods give useful scattered fields from the skin of the aircraft illuminated by an incident plane wave, they largely fail to predict the returns from cavities onboard. As a possible enhancement to these ray-tracing programs, an auxiliary program based on the modal method was developed to predict the scattering of electrically large and complex jet inlets and engines. It is assumed here that these structures can be approximated by a series of rectangular, circular, coaxial and sectoral waveguide sections. Field matching technique is used to give the generalized scattering matrices of the junctions between these waveguide sections. By combining the scattering matrices of the waveguide sections representing the inlet and engine, an overall S-matrix is obtained. Knowing the modes induced at the inlet aperture by the incident wave, the scattered fields from the inlet and engine can be readily predicted in all directions. Such software has been developed. Monostatic RCS measurements of a 0.706m diameter test cylinder containing 30 skewed blades mounted on a centre shaft with a conical hub have been performed at X-band. The dimensions of the structure, the number and orientation of the blades are consistent with existing jet engines. Good agreement between predictions and measurements verify the developed software and analytical method used. This software could generate the database of RCS returns for a given engine over a wide range of aspect angles.

1.0 INTRODUCTION

High range resolution and inverse synthetic aperture radar are promising imaging methods that may be used for non-cooperative recognition of air targets. Both of these methods rely on comparing an observed target return with that from a signature database. It is not practical to generate such a database just from measurements simply because of the large number target types and configurations that have to be tested at a wide range of aspect angles. Further, hostile targets will not willingly submit to such measurements. Hence there is a need for a signature database that is computer generated. Current computer codes are able to predict the electromagnetic scattering from models of aircrafts with varying degree of accuracy that depended very

Paper presented at the RTO SET Symposium on "Target Identification and Recognition Using RF Systems", held in Oslo, Norway, 11-13 October 2004, and published in RTO-MP-SET-080.

much on the precision of the input CAD models. However, none is capable of simulating the significant RCS produced by jet inlets and engines that show up prominently in both HRR and ISAR signatures from in-flight measurements. To rectify this problem, auxiliary software capable of predicting the scattering from jet inlets and engines has been developed. The analysis method used is based on mode or field matching and generalized scattering matrices. Such an approach has been successfully used to treat simple inlet and engine models [2, 4, 5]. The computed scattered fields from the engines can be combined with those from the rest of the aircraft that are calculated using current computer codes to improve on the overall target response. A short description of the method employed is given in section 2. Comparisons of predictions and measurements are carried out in section 3 for a number of configurations. Good agreement is found in most of test cases and conclusion is drawn in section 4.

2.0 MODELLING OF JET INLETS AND ENGINES

A typical scattering problem is shown in Fig. 1 where the inlet is illuminated by an incident plane wave. The waveguide modes induced at the aperture S_g of the inlet are found by field matching [1]. The coefficient, $b_{li}^{(g)}$, of the *i th* guide mode induced by the *l th* space mode is given by

$$b_{li}^{(g)} = -\frac{\sqrt{\eta_i^{(g)}}}{\sqrt{\eta_l^{(s)}}} \iint_{S_g} \bar{e}_i^{(g)*} \bullet \bar{e}_l^{(s)} \, dS$$

This integral can be evaluated analytically for the four combinations between the TE and TM guide mode functions, $e_i^{(g)}$, and the TE and TM space mode functions, $e_l^{(s)}$. The mode impedance is given by η.

Once the induced modes are found, they are propagated into the inlet, which is approximated by a series of uniform waveguide sections. The stepped junctions and waveguide sections are characterized by their generalized scattering matrices, which are cascaded together to give a complete scattering description of the inlet. For a slanted or offset inlet, it is approximated by a series of partially overlapped waveguide sections as shown in Fig. 1. An efficient way of treating the partially overlap stepped junction, which consists of an input waveguide 1, an output waveguide 2 and the in-between common aperture represented as waveguide 0, is to consider all three waveguides together to give a S-matrix characterization of the junction.

$$[S_{11}] = 2\left[P^{(0,1)}\right][W]^{-1}\left[P^{(0,1)}\right]^T - [I] \qquad [S_{12}] = 2\left[P^{(0,1)}\right][W]^{-1}\left[P^{(0,2)}\right]^T$$

$$[S_{21}] = 2\left[P^{(0,2)}\right][W]^{-1}\left[P^{(0,1)}\right]^T = [S_{12}]^T \qquad [S_{22}] = 2\left[P^{(0,2)}\right][W]^{-1}\left[P^{(0,2)}\right]^T - [U]$$

$$[W] = \left[P^{(0,1)}\right]^T\left[P^{(0,1)}\right] + \left[P^{(0,2)}\right]^T\left[P^{(0,2)}\right]$$

$[P^{(0,1)}]$ and $[P^{(0,2)}]$ are the mode coupling matrices between wg. 0 & 1, and wg. 0 & 2 respectively. The coefficients of these matrices are given by the inner products of their mode vectors $\bar{e}_k$, $\bar{h}_k$ as

$$P_{mk}^{(0,1)} = \iint_{S_0} \left[\bar{e}_k^{(0)} \times \bar{h}_m^{(1)}\right] \bullet \hat{z} \, ds \qquad m = 1,.....,M \qquad k = 1,.....,K$$

$$P_{nk}^{(0,2)} = \iint_{S_0} \left[\bar{e}_k^{(0)} \times \bar{h}_n^{(2)}\right] \bullet \hat{z} \, ds \qquad n = 1,.....,N \qquad k = 1,.....,K$$

where there are K modes in waveguide 0, M modes in waveguide 1, and N modes in waveguide 2. These integrals may be evaluated analytically. *[U]* and *[I]* are unit matrices. The number of modes used in each waveguide section is set by the maximum cutoff wave number specified.

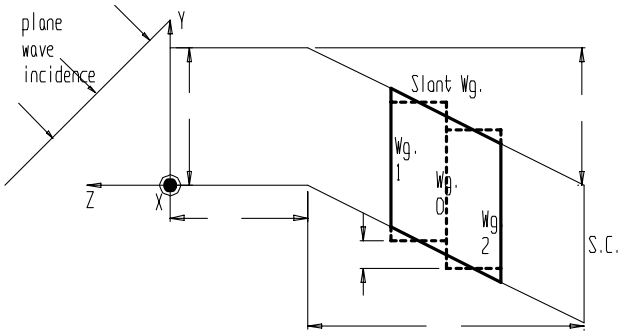

Fig. 1 Plane wave illumination of jet inlet

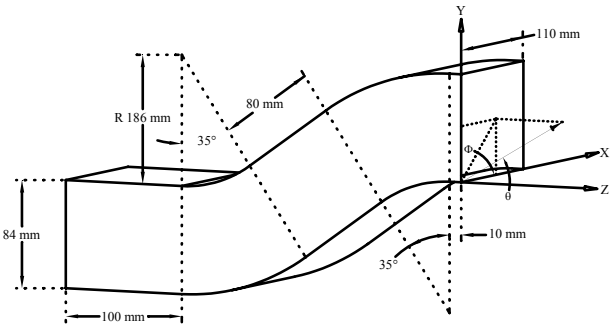

Fig. 2 S-shape Inlet

The general waveguide software was used to analyze the S-shape inlet of Fig. 2. Very good correlation is found between theory and measurement as demonstrated in [2]. Displacement steps between waveguide sections no larger than 0.1λ are sufficient to model a smooth curve inlet. At the end of the rectangular inlet, it transitions into a circular conical cylinder where the engine is located. Modal characterization of the rectangular to circular transition has also been developed. For the present paper, we will concentrate on the modelling of the engine with skewed blades.

The circular cylinder of the engine with the centre shaft is treated as a coaxial waveguide. Both the centre and outer conductors may be varying to represent a conical engine compartment. The centre hub is modelled by a series of stepped centre conductors. The blades mounted on the centre shaft, as shown in Fig. 3, are inclined at an angle with the axis of the engine.

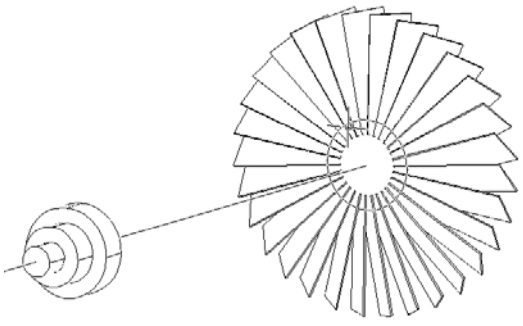

Fig. 3 Skewed blades and centre hub

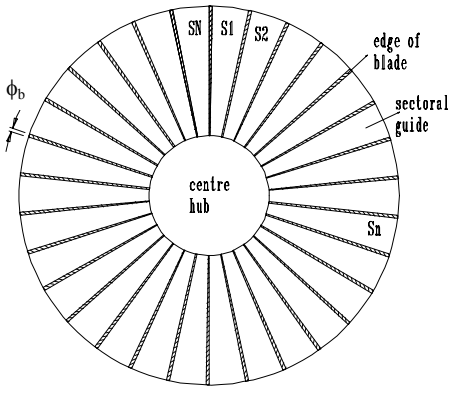

Fig. 4 Coaxial guide – blade junction

The generalized S-matrix characterization of the junction between coaxial waveguide and sectoral waveguides is found by field matching. This formulation is given by Chan [3]. The channel between a pair of skewed

blades is approximated by a slanted or curved sectoral waveguide, which is divided into a number of axially, translated and azimuthally rotated short straight waveguide sections. The S-matrix between two displaced sectoral waveguide sections are defined by the same matrix equations given above for partially overlapped rectangular waveguides. The difference here is the coupling integral can be evaluated in close form only for the azimuthal Φ variable. The integration along the radial direction must be done numerically. Recursive combination of this junction S-matrix and that of the adjacent straight section yields the resultant S-matrix of the slant blade channel. Thus a single stage of blades can now be characterized by the back-to-back combination of a coaxial waveguide to multiple sectoral waveguide junction interconnected by sections of slanted sectoral waveguides.

The S-matrix of the blades need only be computed once. If the blades are rotated, the resultant S-matrix is obtained through a transformation of the non-rotated matrix. A local coordinate system is attached to the blades and it rotates with them. For a complete representation of the fields both the V- and H- sets of modes in the local coordinate system are required. The analysis of the blades is carried out with these local sets of modes. A global coordinate system is placed at the aperture of the engine. The modes resulting from the plane wave illumination are expressed in the global coordinate system. The local system is rotated with respect to the global system by an angle ϕ_0. Because of mode orthogonality, the global TE (TM) V- or H- mode is resolved only into the local V'- and H'- types of TE (TM) mode. The transformation between the global incident modes (a^V, a^H) and the local incident modes ($a^{V'}$, $a^{H'}$) is simply given by

$$\begin{bmatrix} a^{V'} \\ a^{H'} \end{bmatrix} = \begin{bmatrix} C_{11} & C_{12} \\ C_{21} & C_{22} \end{bmatrix} \begin{bmatrix} a^{V} \\ a^{H} \end{bmatrix}$$

Here C_{11} and C_{22} are diagonal matrices with diagonal elements given by $\cos(m\phi_0)$, where m is the mode first index. C_{12} and C_{21} are rectangular matrices because certain modes are present in the V- set and not in the H- set. For instance, the TE_{0n} modes belong to the H-set only while the TM_{0n} modes are in the V-set only. The non-zero entries of C_{12} are given by $\sin(m\phi_0)$ for TM modes and $-\sin(m\phi_0)$ for TE modes. The non-zero elements of C_{21} are given by $-\sin(m\phi_0)$ for TM modes and $\sin(m\phi_0)$ for TE modes. If the reflection matrix of the blades in the local coordinate system is denoted by S_{11}, then the corresponding matrix in the global system is obtained from the transformation $C^T S_{11} C$, where T indicates transposition.

The S-matrices of various stages of blades and the inlet are combined to give the overall scattering parameters characterizing the jet engine. It should be mentioned that both propagating and evanescent modes are used in the field matching to model accurately each junction or structural change. However, only those accessible evanescent modes above a specified threshold are used for the S-matrix combination of the various junctions. This reduces significantly the order of the matrices involved in the computations. Knowing the S-matrix of the engine and the incident modes, the reflected modes at the inlet aperture are readily obtained. Using Kirchoff's diffraction integral, the scattered fields of the aperture modes in all directions are determined analytically.

3.0 VALIDATION OF MODEL

A test cylinder of 0.706 m diameter was fabricated out of metal ventilation duct. A centre shaft of diameter 0.224 m carrying 30 equally spaced blades that are inclined at 45° (stagger angle) to the longitudinal axis is placed inside the cylinder. The axial length of the blade region is 7.62 cm. At the back, the shaft extends 7.30 cm beyond the blade region and terminates into a circular shorting plate, which also forms the supporting structure. At the front of the shaft, a smooth conical hub of 0.164 m axial length is attached. There is an air

gap of 0.5 cm between the end of the blade and the cylinder wall. This facilitates the rotation, axial translation and placement of the blade assembly in an off circular enclosure. The blades are made out of 0.159 cm thick aluminum plates. The blades in the actual fabricated assembly are not identical and they are not normal to the shaft surface. A picture of the cylinder and blade assembly mounted for measurement is shown in Fig. 5. Absorbers were placed around the supporting structure to reduce external reflections.

Fig. 5 Test cylinder with skewed blade assembly

In our idealised approximation of this blade assembly, the blades extend all the way to the wall i.e. there is no air gap, and the blades are always normal to the shaft surface and cylinder wall. The constant thickness of the blade is replaced by a sectoral wall of included angle 0.373°. A sectoral guide of angle 11.627° then represents the blade channel. The twist angle of the blade, defined as the difference in the projected azimuthal ϕ-angles of the front and back edges of the blade, is 39.01°.

All the measurements reported here were taken at the DRDC outdoor test facility [7] using a pulsed radar with 200ns pulse width and 1KHz PRF. The cylinder was placed 125m away. The illuminating beamwidth was 2° AZ x 6° EL. The transmitting and receiving beams were horizontally polarized and only azimuth cuts were made. Hence all the measured monostatic scattered responses are for TM incidence. First, a conducting flat plate was placed at 1 m and 1.91 m inside the cylinder. The measured H-H RCS of the cylinder terminated with a flat plate is plotted in Figs. 6 and 7 for the two plate locations together with the predictions at 8.9 GHz. The data, normalized to the peak at boresight, are shown from -60° to +60° in the azimuth plane. As can be seen, the agreement between measurement and prediction is very good in both cases. There is extraneous reflection from the side or mounting support at the near-in angles and the test article is not symmetrical.

Next, the cylinder with the blade assembly is modelled and tested. In modal analysis, sufficient number of modes must be used to obtain result convergence. To treat the slanted blade channel, 2664 sectoral waveguide modes are used, with the highest approximating mode cutoff wavenumber $k_c = 6.5k_0$ where k_0 is the operating wavenumber. To represent the fields in the circular waveguide and coaxial waveguide regions, it is found that only modes with mode cutoff wavenumber less than $1.3k_0$ need be used. This is demonstrated in Fig. 8, where the RCS of the cylinder with the blade assembly is shown for the cases with $1.3k_0$ and $1.7k_0$ highest mode

cutoff wavenumber. Only small differences are observed between them. Plotted in Fig. 9 is the RCS at 8.9 GHz of the cylinder and blades with two different types of nose cones, 4-step and 6-step hubs of axial lengths 0.21m and 0.164m. These responses are for TE incidence and are more or less the same with minor changes.

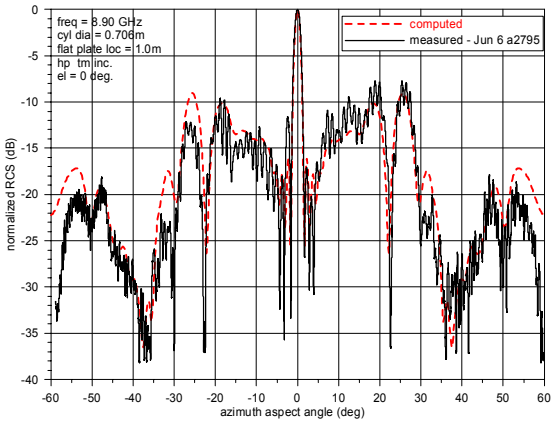

Fig. 6 RCS of cylinder with flat plate at 1m

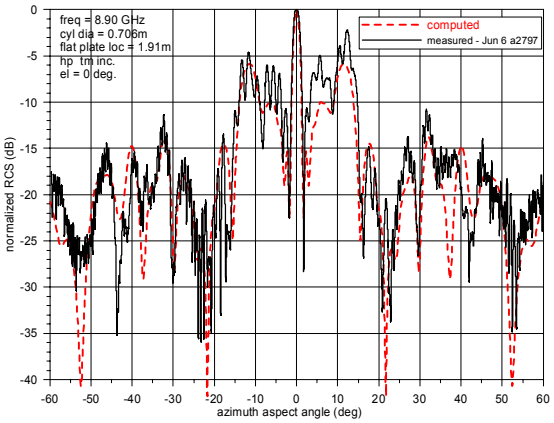

Fig. 7 RCS of cylinder with flat plate at 1.91m

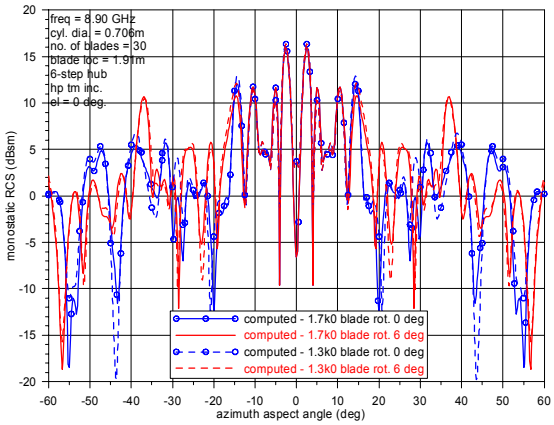

Fig. 8 RCS convergence of cylinder with different number of modes

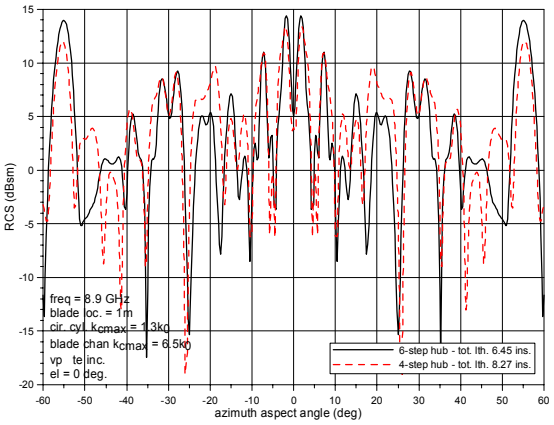

Fig. 9 RCS of blades with different centre hubs

Very often in the RCS modelling of the aircraft, the complexity of the blades in the engine is replaced by a flat plate at the same location. The consequences of this simplification can be seen in Figs. 10 and 11. Here the RCS of the cylinder with flat plate, flat plate with nose cone and skewed plates located 1m and 1.91m from the aperture are plotted for comparison at 8.9 GHz. At boresight, where there is a peak value for the flat plate with and without the nose cone, a null is observed for this particular inclined blades configuration. This is caused by the conversion of the lowest order TE_{11} mode, which carries the most power, into the propagating higher order modes by the single stage of blades. These higher order modes have maximum radiation in different off boresight directions. As a result, the peak backscatter field off axis for the blade assembly is approximately 14 dB below the on-axis maximum of the flat plate, which has been confirmed through measurement. The RCS of the skewed blades is also lowered by approximately the same amount at the other off normal aspect angles. Thus there is substantial error in the simplified model of this engine. Addition of a centre hub to the flat plate causes change only at the near-in aspect angles.

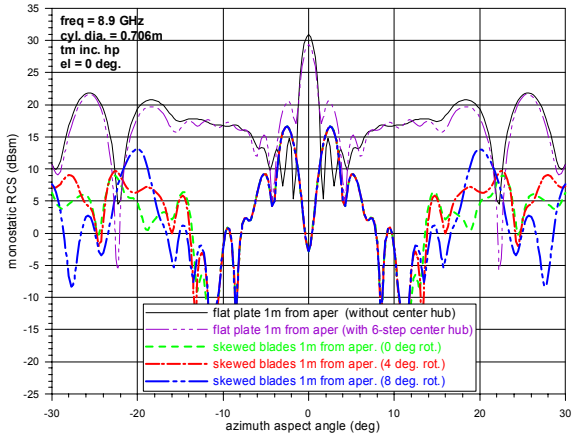

Fig. 10 RCS of cylinder with obstacle at 1m

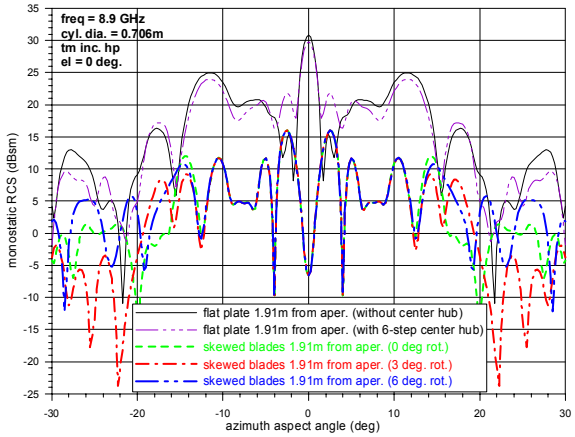

Fig. 11 RCS of cylinder with obstacle at 1.91m

The RCS of the cylinder containing the blade assembly with a smooth conical center hub was measured at 8.9, 9.1 and 9.2 GHz for TM incidence. The blades were placed at two locations, 1m and 1.91m from the aperture. The test data are normalized to the peak response and are plotted in Figs. 12 to 17 for azimuth aspect angles ranging from -60° to +60°. Shown on plots are the predicted RCS for comparison. The center conical hub of 0.163m axial length is approximated by a 6-section center conductor. The diameter of each section is 0.045m, 0.113m, 0.155m, 0.184m, 0.206m and 0.224m. For the circular guide and coaxial guide discontinuities, the highest cutoff wavenumber of the field approximating modes is $1.7k_0$. To represent the fields, the number of circular waveguide modes used is 6268. The number of coaxial guide modes in the respective hub section is 6252, 6108, 5964, 5852, 5744 and 5648. The blade channel field distribution is approximated by 2664 sectoral guide modes. The total memory requirement by the program is 3.6 GB. Each frequency run for any number of aspect angles and polarization states takes about 23 hours on a Sunblade 2000 running at 900MHz. It is possible to reduce the run time by decreasing the number of modes in the various regions with some impact on the computed scattered fields. It should be mentioned that this execution time is at least one to three orders of magnitude faster than existing ray-based or finite element based cavity analysis programs [6] that produce results with questionable accuracy for complex blade arrangement.

When comparing the measurements with the predictions, one should bear in mind that the measured data is a lot noisier due to a drop of 14 dB in the scattered power from the cylinder with the blades. At the test facility, the cylinder is mounted on an azimuth turntable. It is not possible to align the cylinder in elevation with the transmit/receive antenna. This misalignment will cause the two lobes on either side of the boresight direction to become asymmetrical, which is clearly evident here. Further, the computer model is an approximate representation of the test article, in that the air gap at the tips of the blades is ignored and all the blades are not the same. The computed results deal solely with the internal scattering of the cylinder and do not include the reflected fields from the outside of the cylinder or support structure, which is covered by flat absorbing sheets. Such external reflections cannot be eliminated from the measurements. Still, with the coincidence of the major lobes in both amplitude and direction, it can be said that there is fairly good agreement between the test and computed data.

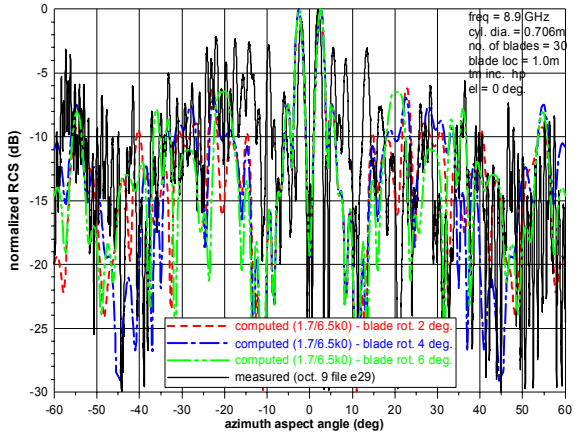

Fig. 12 RCS of cylinder with blades at 1m - 8.9 GHz

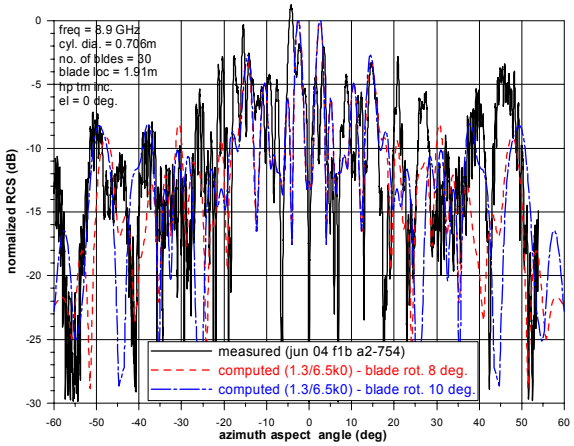

Fig. 13 RCS of cylinder with blades at 1.91m - 8.9 GHz

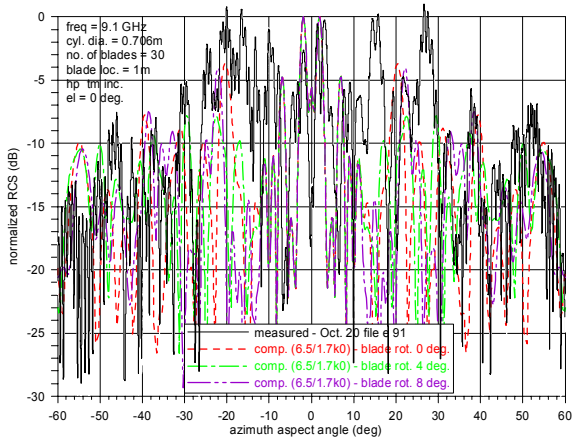

Fig. 14 RCS of cylinder with blades at 1m - 9.1 GHz

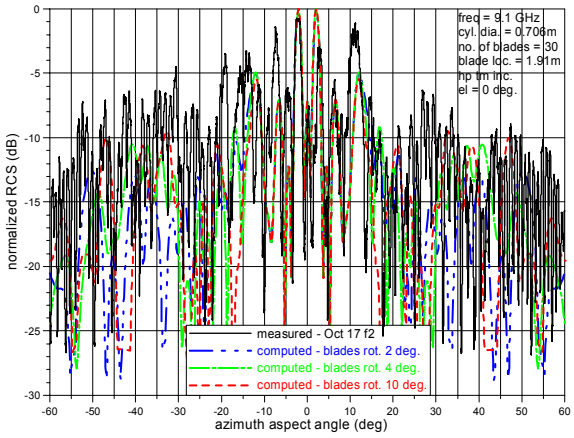

Fig. 15 RCS of cylinder with blades at 1.91m - 9.1 GHz

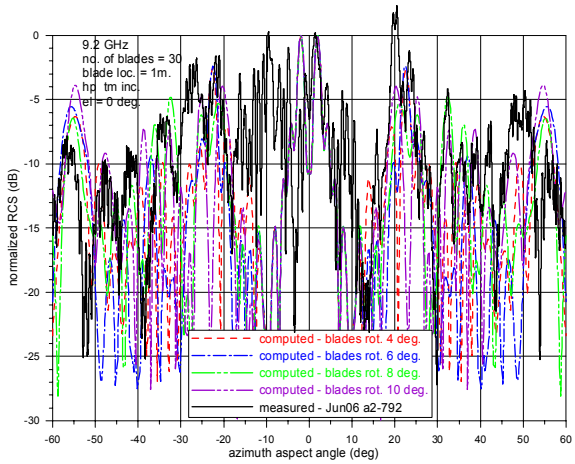

Fig. 16 RCS of cylinder with blades at 1m - 9.2 GHz

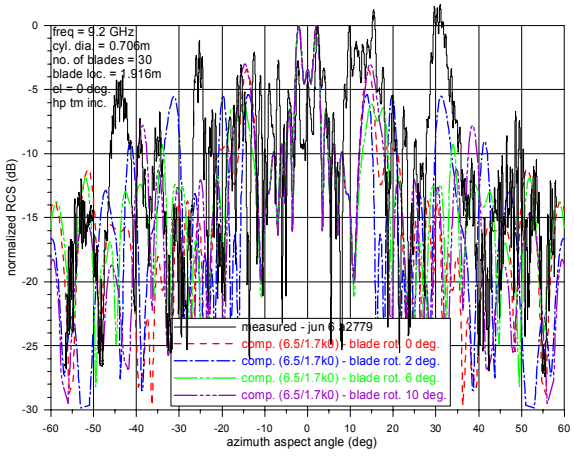

Fig. 17 RCS of cylinder with blades at 1.91m - 9.2 GHz

4.0 CONCLUSION

A procedure based on modal analysis has been presented for the analysis of jet inlets and engines. The complex geometry of a center hub and shaft with inclined blades is successfully treated. A test cylinder with a skewed blade assembly has been built and tested at X-band. Dimensions of the cylinder and blades are similar to those of the present day jet engines. The measured amplitudes of the backscatter fields agree well with the computer simulations. Even though a large number of modes are required for field representation in the cylinder and blade assembly, present day desktop computers can readily handle the computation workload and memory requirement. In this development, canonical waveguide sections are utilized to model the engine so that internal fields can be approximated by analytical modes. Similar modal approach may also be applied to non-standard engine and inlet cross-sections, where numerical modes that meet the boundary conditions are employed instead to provide efficient calculation of their RCS.

5.0 REFERENCES

[1] K.K. Chan and F. Tremblay: "Scattering from rotating blades in a cylinder", International Conference on Radar, Paris, France, May 1994, pp. 83-88.

[2] K.K. Chan and Silvester Wong: "Modal Approach to RCS Computation of Electrically Large Inlets", IEEE AP-S International Symposium, San Antonio, June 2002, Vol. 3, pp.114-117.

[3] K.K. Chan and F. Tremblay: "Mode matching analysis of metallic blades in a cylinder", IEEE AP-S International Symposium, Newport Beach, June 1995, Vol. 1, pp. 38-41.

[4] Anastassiu H.T. et. al., "Electromagnetic Scattering from Simple Jet Engine Models", IEEE Trans. on Ant. & Prop., 1996, Vol. 44, No.3, pp. 420-421

[5] Anastassiu H.T. and Volakis J.L.; "The Modal Matching Technique for Electromagnetic Scattering by Cylindrical Waveguide with Canonical Terminations", IEEE AP-S International Symposium, 1995, Vol. 3, pp. 26-29

[6] K.K. Chan and Silvester Wong: "Accurate RCS Prediction of Electrically Large Jet Inlets and Engines", Twelfth Intern. Conf. on Ant. & Prop., ICAP 2003, U.K., April 2003, Vol. 1, pp.253 - 256.

[7] S. Wong, E. Riseborough and G. Duff: "Experimental facility for measuring aircraft inlet/engine radar cross section", RTO-SET 080 Fall 2004 Symposium, Oslo, Norway, October 2004.